Original Article

Histopathologic evaluation system of African swine fever in wild boar infected with high (Arm07) and low virulence (Lv17/WB/Riel) isolates

Veterinary Pathology
1–15

DOI: 10.1177/03009858241266944
journals.sagepub.com/home/vet
Sage

Néstor Porras[1], José M. Sánchez-Vizcaíno[1,2], José Á. Barasona[1,2], Alberto Gómez-Buendía[1], Estefanía Cadenas-Fernández[1,2], and Antonio Rodríguez-Bertos[1,3]

Abstract

To understand the clinicopathological forms of African swine fever (ASF) in wild boar, it is crucial to possess a basic knowledge of the biological characteristics of the currently circulating ASF virus isolates. The aim of this work is to establish an accurate and comprehensive histopathologic grading system to standardize the assessment of the ASF lesions in wild boar. The study evaluated the differences between animals infected with a high virulence genotype II isolate (Arm07) (HVI) through intramuscular (IM) (n = 6) and contact-infected (n = 12) routes, alongside those orally infected with a low virulence isolate (Lv17/WB/Riel) (LVI) (n = 6). The assessment included clinical (CS), macroscopic (MS), and histopathologic (HS) scores, as well as viral loads in blood and tissues by real-time quantitative polymerase chain reaction (qPCR). Tissues examined included skin, lymph nodes, bone marrow, palatine tonsil, lungs, spleen, liver, kidneys, thymus, heart, adrenal glands, pancreas, urinary bladder, brain, and gastrointestinal and reproductive tracts. The HVI group exhibited a 100% mortality rate with elevated CS, MS, and HS values. Animals infected by contact (CS = 12; MS = 58.5; HS = 112) and those intramuscularly infected (CS = 14.8; MS = 47; HS = 104) demonstrated similar values, indicating that the route of infection does not decisively influence the severity of clinical and pathological signs. The LVI group showed a 0% mortality rate, an inconspicuous clinical form, minimal lesions (CS = 0; MS = 12; HS = 29), and a lower viral load. Histopathologic evaluation has proven valuable in advancing our comprehension of ASF pathogenesis in wild boar and paves the groundwork for further research investigating protective mechanisms in vaccinated animals.

Keywords

African swine fever virus, high virulence isolate, histopathologic evaluation, low virulence isolate, scoring system, vaccine, wild boar

African swine fever (ASF) is a hemorrhagic disease included in the World Organization for Animal Health (WOAH) list of notifiable diseases[40] that affects domestic pigs and wild boar (*Sus scrofa*).[34,36] The causative agent is the only member of the genus *Asfivirus* in the *Asfarviridae* family.[1] ASF is a serious socio-economic and health threat to the global swine sector.[31] Control strategies are based on early detection of outbreaks, followed by the application of strict sanitary measures.[2,13,35,36] Vaccination is the optimal strategy to prevent and control the ASF epidemic; however, an ASF vaccine with high immunoprotective potential still remains to be explored.[42] At present, 2 live attenuated vaccines against ASF have been officially approved for domestic use in pigs in Vietnam.[9,42] Currently, part of Eastern and Central Europe remains infected, affecting both domestic pigs and wild boar,[33,40,41] with the latter playing a key role in the spread and maintenance of the virus in neighboring regions of the European Union.[8,33]

Gaps remain in the basic knowledge of the biological and immunological characteristics of currently circulating ASF virus (ASFV) isolates.[2] This information is necessary to understand the pathogenic mechanisms and to characterize the pathological forms caused by these isolates.[32] Macroscopic examination of the dead animals is an essential source of information and early diagnosis,[22,27] particularly in the wild boar population, where the emergence of ASFV in new areas is characterized by the presence of carcasses in the field.[39] This is

[1]VISAVET Health Surveillance Centre, Complutense University of Madrid, Madrid, Spain
[2]Department of Animal Health, Faculty of Veterinary Medicine, Complutense University of Madrid, Madrid, Spain
[3]Department of Internal Medicine and Animal Surgery, Faculty of Veterinary Medicine, Complutense University of Madrid, Madrid, Spain

Supplemental material for this article is available online.

Corresponding Author:
José Á. Barasona, VISAVET Health Surveillance Centre, Complutense University of Madrid, Avenida Puerta de Hierro, s/n, Madrid, 28040, Spain.
Email: jbarason@ucm.es

particularly important for the study of natural infections in the field, as it provides a more realistic expression of the disease that can be evaluated from a practical perspective.[33,37]

Most of the macroscopic findings have been described following experimental infection in wild boar.[27] These findings do not differ significantly from those observed in a natural environment.[37] However, it is important to point that in the natural environment, there are uncontrollable factors that may affect the severity of the lesions (e.g., mixed infections with different strains, climatological conditions, the health and immunological status of the animals, and heterogeneity of the populations in terms of age, sex, and nutrition).[33] In addition, under field conditions, a proper diagnosis and timely intervention is essential for histopathologic studies as they might be hampered by an advanced stage of decomposition.[20] For these reasons, experimental studies are essential for controlling these factors so that a standardized evaluation of clinical signs and gross and histopathologic findings can be made.

Review papers and experimental studies in both domestic pigs and wild boar, with different isolates and routes of administration, have gradually described the pathogenic characteristics of ASF, observing certain differences in clinical outcomes and severity of lesions.[6,11,12,22,27,33,34] It has been confirmed that there is a direct relationship between the virulence of the virus and the pathological course.[28,34] However, other factors such as dosage, route of administration, age, and the immunological status of the host may also play key roles in the clinical evolution of the disease.[6,17,25,30] Histopathology is a necessary tool to evaluate the relationship between the factors involved in the pathogenic process and the presentation of the disease. Furthermore, it is essential to study of the dynamics of certain low virulence isolates as possible vaccine candidates,[14] in order to assess their efficacy and safety.[4,5]

Until now, few studies have described and graded the ASF histopathologic lesions in wild boar,[21,37–39] which were based on the parameters established by Galindo-Cardiel et al[12] in domestic pigs. In this study, we evaluated the presence and severity of the microscopic lesions in wild boar infected with a highly virulent isolate (Arm07), and a naturally attenuated isolate (Lv17/WB/Rie1) genotype II ASFV, which has demonstrated its potential to produce an immune response in both domestic pigs and wild boar.[4,5,15] Furthermore, we evaluated factors that may be related to the presence and severity of lesions including the isolate virulence, route of administration, dosage, survival time in terms of days post-infection (dpi), viral loads (blood and tissues), clinical signs, and pathological form (acute, subacute, chronic). To achieve this purpose, we designed detailed histopathologic evaluation criteria with a specific scoring system that was adapted to wild boar, covering a total of 19 organs.

Material and Methods

Animals and ASFV Isolates

The animal collection used in this study, were obtained from previous experiments.[4,5,27] All experiments were performed under biosafety level 3 conditions at the VISAVET Center at the University Complutense of Madrid, in accordance with European, national, and regional regulations and approved by the Ethics Committee of the Comunidad de Madrid (reference PROEX 124/18). Thirty female wild boar piglets, aged 3-4 months and weighing 10-15 kg, were obtained from a commercial wild boar farm, which tested negative for the following main porcine pathogens in the region: *Mycobacterium bovis*, *Mycoplasma hyopneumoniae*, suid herpesvirus 1, and porcine circovirus type 2. Details of the virus isolates and antibodies detection against ASFV can be found elsewhere.[4,5] The specific details of each animal are shown in Supplemental Table S1.

Experimental Design

Three groups were included in this study: high virulent ASFV isolate (HVI) group, low virulent ASFV isolate (LVI) group, and a negative control group. The HVI group consisted of 18 animals, 6 of which were infected intramuscularly (IM) with 10 median hemadsorption units (HAD_{50}) of a highly virulent isolate (Arm07) (shedder animals) and the remaining 12 animals were infected by exposure to the shedder animal group (shedder-pig exposure infection model). Animals in the HVI group were kept up to 15 dpi and were slaughtered when they reached the endpoint criteria (clinical score [CS] $\geq$ 18). The LVI group consisted of 6 animals orally infected with 10^4 median tissue culture infective dose ($TCID_{50}$) of the low virulence isolate Lv17/WB/Rie1 of naturally attenuated ASF virus, which has been demonstrated to induce an immune response in both domestic pigs and wild boar.[15] Animals in the LVI group were maintained for 30 days to allow the development of an immune response before humane sacrifice. The negative control group was composed of 6 archival healthy animals, not infected/inoculated with any ASFV isolate, and not housed simultaneously. Specific details of the experimental design are shown in Fig. 1.

Clinical Evaluation

Animals were observed daily throughout the study to monitor their health status by a video camera (recording 24 hours a day) and visits by a wildlife-specialist veterinarian. The evolution of the ASFV infection was assessed using a quantitative CS in accordance with specific parameters for ASFV infection in wild boar described by Cadenas-Fernández et al.[7] All clinical observations were daily recorded, except temperature, to minimize animal handling and stress. The humane endpoint for this study was predefined as animals with a CS $>$ 18. In addition, inclusion criteria involved animals manifesting severe clinical signs at level 4 intensity, which included fever, altered behavior, compromised body condition, and persistent respiratory and digestive symptoms for more than 2 consecutive days. These criteria were tailored to conform with the guidelines outlined in the previously published study (Supplemental Table S2).[7] Furthermore, euthanasia was considered for animals enduring unacceptable conditions, as determined by veterinarian criteria, irrespective of whether they reached the predefined humane endpoint. For this study, only the CS obtained on the last day (day of sacrifice) was considered.

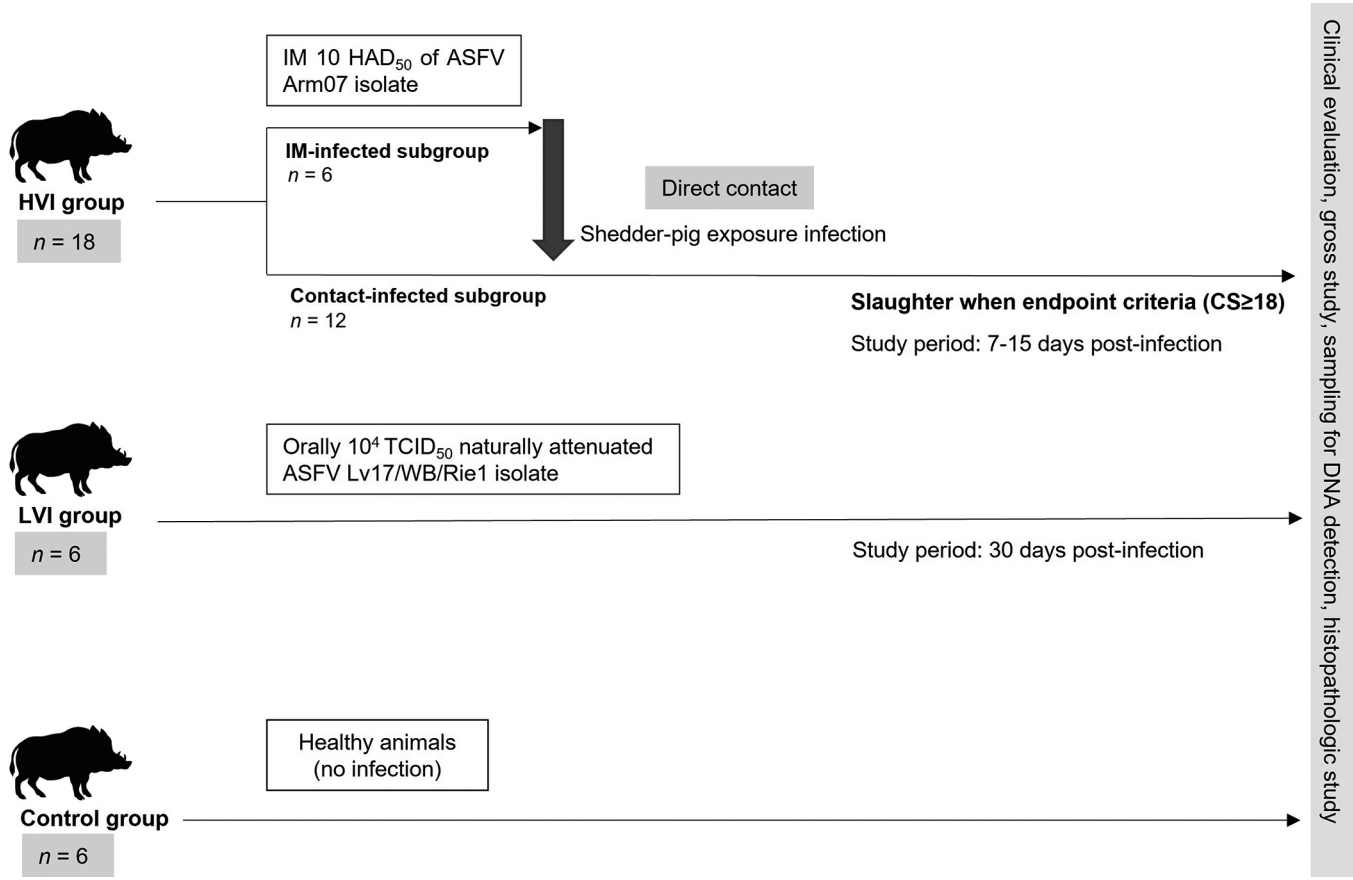

Figure 1. Scheme of the study design including the 3 groups (high virulent isolate [HVI], low virulent isolate (LVI), and control group), from prime inoculation to the end of the experiment. All groups included in the experimental design underwent clinical evaluation, gross study, sampling for DNA detection, and histopathologic study. IM, intramuscular; HAD_{50}, median hemadsorption units; ASF, African swine fever; $TCID_{50}$, median tissue culture infective dose; CS, clinical score.

Real-Time Quantitative Polymerase Chain Reaction (qPCR)

During the postmortem examination, we collected samples of blood and a selection of 17 tissues. Seven of these were lymph nodes (renal, mediastinal, retropharyngeal, mesenteric, gastrohepatic, inguinal, and submandibular), as well as palatine tonsils, lungs, heart, liver, spleen, kidneys, urinary bladder, intestine, bone marrow, and brain. To validate the presence of the ASFV genome in these samples, DNA extraction was carried out using the High Pure PCR Template Preparation Kit (Roche Diagnostics GmbH, Roche Applied Science, Mannheim, Germany). In brief, 10% (w/v) clarified homogenized tissue suspensions or blood samples were prepared in phosphate-buffered saline. The detection of the ASFV DNA in blood and tissue samples was performed using the Universal Probe Library (UPL) qPCR recommended by the WOAH and previously described by Fernández-Pinero et al.[10] Based on the DNA sequence of the VP72 coding genome region of ASFV (GenBank accession no. S89966), the primers were prepared at a concentration of 20 pmol/μL, with the forward primer sequence being 5′-CCC-AGG-RGA-TAA-AAT-GAC-TG-3′ (ASF-VP72-F) and the reverse primer sequence being 5′-CAC-TRG-TTC-CCT-CCA-CCG-ATA-3′ (ASF-VP72-R). According to WOAH manual, qPCR protocol was optimized using LightCycler480 Probes Master kit (Roche Applied Science). Positive qPCR results were determined by identifying the cycle threshold (Ct) values at which reporter dye emission appeared above the background within 40 cycles. For this study, only the blood ASFV Ct values obtained on the last day (day of slaughter) were considered. Positive and negative controls were used in DNA extraction and in qPCR. As a positive control, we have used well known and sequenced sample of the virulent ASFV isolate, and as a negative control nuclease-free sterile water.

Gross Evaluation of ASFV Lesions and Sampling

During postmortem survey, macroscopic lesions were evaluated and scored following a previously published protocol of Rodríguez-Bertos et al.[27] For this study, tissue samples were taken from the following organs and fixed in 10% neutral-buffered formalin: lungs (cranial, middle, caudal, and accessory lobes), spleen, liver, kidneys (cortex, medulla, and renal pelvis), lymph nodes (cortex and medulla), bone marrow (red portion), palatine tonsil, thymus, heart (epicardium, myocardium, endocardium, and atrioventricular valve), adrenal glands, urinary bladder, gallbladder, pancreas (head, body, and tail), stomach (cardia, fundus, corpus, and pyloric antrum), small

intestine (duodenum, jejunum, ileum, and ileocecal valve), large intestine (cecum, colon, and rectum), central nervous system (cerebrum and cerebellum), reproductive system (ovaries, uterine ducts, and uterine body), and skin. Moreover, the area of lesion with the highest severity was always sampled, incorporating a margin of healthy tissue when feasible. Same methodology was followed during trimming, making the cut in the most affected area, and then consecutive sections were made with the less affected areas (obtaining 3 cassettes of the same organ). Several lesions/parameters were assessed based on the organ/tissue affected, resulting in a total of 30 lesions/parameters evaluated in each animal. These lesions were semi-quantitatively scored as follows: normal (0), mild (1), moderate (2), and severe (3). With this method, the total macroscopic score (MS) for each animal was calculated as a sum of each parameter in a 0-90 grading scale.

Histopathologic Evaluation

The protocol of Galindo-Cardiel (2013) was used as a guide,[12] and new histopathologic findings observed in our work and in previous studies in wild boar were added.[21,37–39] Thus, in addition to the 4 main organs previously studied (lungs, spleen, liver, and kidneys),[12] other organs were included (lymph nodes, bone marrow, palatine tonsil, thymus, heart, adrenal glands, pancreas, urinary bladder, gastrointestinal tract, central nervous system, reproductive tract, and skin). Thus, the expanded biobanking effort allowed the establishment of a more precise and comprehensive histopathologic evaluation specifically adapted for wild boar. Several lesions/parameters were assessed based on the organ/tissue affected, resulting in a total of 80 lesions/parameters evaluated in each animal. These lesions were semi-quantitatively scored as follows: normal (0), mild (1), moderate (2), and severe (3). With this method, the total histopathologic score (HS) for each animal was calculated as a sum of each parameter in a 0-240 grading scale. The criteria followed for histopathologic assessment and scoring of each organ studied are described in detail in Supplemental Tables S3-S20. For a more comprehensive assessment of the lesion severity in each organ, all lesions (including vascular, inflammatory, and degenerative parameters) were systematically summarized. In this manner median values were calculated for each examined organ, employing a grading scale of 0 to 3 (Supplemental Table S21). Histopathologic images of each organ according to the scoring system are shown in Supplemental Figures S1-S16.

Statistical Analyses

Animal CS, MS, and HS, along with the Ct values for the blood and all of the tissues evaluated, were compared between groups. Moreover, statistical differences between the HS of each parameter were assessed. Analyses were performed using a Kruskal-Wallis (K-W) test followed by a Dunn's test for pairwise multiple comparisons with a Holm adjusted method as a post hoc test. Also, to assess any differences between HVI subgroups (ie, IM-infected and contact-infected), a Mann-Whitney (M-W) test was performed.

Pearson's correlation coefficient was used to assess the relationship between animal HS/MS and the dpi in the HVI subgroups. Likewise, animal HS results were correlated with the data obtained for MS, CS, and Ct (blood); tissue HSs were correlated with the MS and Ct of each tissue, and the HS was correlated with the MS of each parameter. All statistical analyses were performed in R.[26]

Results

Viral Loads in Blood and Tissue Samples

On the day of sacrifice, the HVI group showed high viral loads in blood, mean Ct = 18.9; 95% confidence interval (CI): 17.3-20.4. No differences were observed between subgroups (M-W test: $P = .43$). In addition, ASFV was detected in all tissues (Ct = 22.7; 95% CI: 22.2-23.1). The LVI group showed low viral loads in blood at 34 dpi (Ct = 34.3; 95% CI: 29.2-39.5). Only 1 wild boar in the LVI group (case 19) tested positive in all tissue samples (Ct = 33.4; 95% CI: 32.5.2-34.3). The remaining animals in the LVI group tested positive for qPCR (Ct = 34.92; 95% CI: 34-35.8) in 9 tissues, including lymph nodes (submandibular, retropharyngeal, inguinal, and mediastinal), lungs, spleen, kidneys, synovial membranes, and brain. The control group showed no signs of viremia, and no ASFV was detected in their tissues.

Statistically significant differences in viral loads (both in blood and tissues) were observed between groups (K-W test: $P < .0001$). The post hoc analysis revealed significant differences between the HVI group and LVI and control groups (Dunn's test: $P < .01$), but not between the LVI and control groups (Dunn's test: $P < .01$). Individual Ct values (blood and tissues) are shown in Fig. 2.

Clinical and Gross Evaluations

Animals in the HVI exhibited clinical signs compatible with ASF including elevated body temperature, reduced alertness, ambulatory challenges, widespread erythema, mild ocular discharge, and digestive signs including the presence of mucus in stools and sporadic vomiting. No differences in CS were observed (M-W test: $P = .2$) between IM-infected (CS = 14.8; 95% CI: 11.9-17.8) and contact-infected animals (CS = 12.5; 95% CI: 10.1-14.9), with substantial individual variation in CS values. Two IM-infected animals were euthanized at 7 dpi based on the humane endpoint criteria. The remaining succumbed to the disease before reaching the humane endpoint (7-12 dpi). Of the 12 contact-infected animals, 10 were euthanized between 12 and 15 dpi, while the remaining 2 died during the same period. No relevant clinical signs were observed in animals from the LVI and control groups, except for 1 LVI animal that experienced temporary fever. Significant differences were observed in CS between the HVI and LVI groups, as well as between the HVI and control groups (K-W test: $P < .0001$),

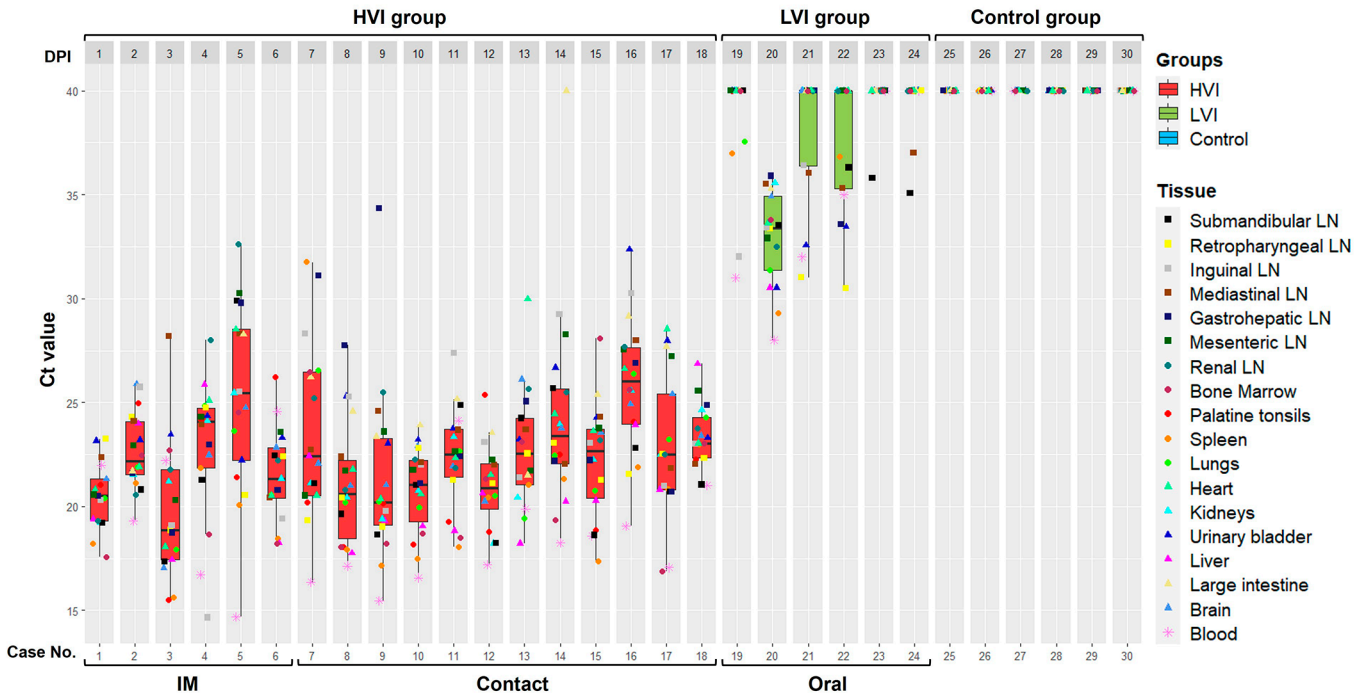

Figure 2. African swine fever virus Ct (cycle threshold) values (tissues and blood) obtained in each group, high virulent isolate (HVI) = red color; low virulent isolate (LVI) = green color; control = blue color. Boxes indicate the interquartile range, middle highlighted bars inside boxes indicate median values, and the top and bottom of the box indicates the 75th and 25th percentile. Whiskers denote 97.5th and 2.5th percentile. LN, lymph node; IM, intramuscular.

but no differences were found between the LVI and control group (Dunn's test: $P > .05$). Individual CS and MS values are shown in Fig. 3a.

The main necropsy findings in HVI group were moderate to severe ascites, hydrothorax, and hydropericardium. Boars had pulmonary edema, congestion, and multifocal subpleural hemorrhages in the pulmonary parenchyma. Congestion and enlargement of the spleen (splenomegaly), liver (hepatomegaly), and lymph nodes (lymphadenomegaly) were evident. Hemorrhages of varying severity were frequently observed in the lymph nodes and kidneys, and occasionally in the thymus, heart, urinary bladder, adrenal gland, pancreas, and gastric and intestinal mucosa (Fig. 3b). In this case, a higher MS was observed in the contact-infected (MS = 58.5; 95% CI: 52.9-64.2) compared to the IM-infected animals (MS = 47; 95% CI: 41.8-52.2) (M-W test: $P = .04$). Furthermore, there was a positive correlation between MS and dpi in HVI-infected animals, indicating that MS values tend to increase as dpi elapses, Pearson correlation coefficient (r) = 0.75, 95% CI: 0.44-0.90.

Necropsy findings for the LVI group at 34 dpi revealed mild gross lesions (MS = 11.8; 95% CI: 8.5-15.2). Animals presented hyperemic splenomegaly (with a white pulp hypertrophy), hepatomegaly with congestion, and multifocal subpleural petechial hemorrhages in the lungs (Fig. 3c). The control group did not display relevant gross lesions (MS = 3.8; 95% CI: 2.9-4.8). Significant differences were observed in MS between the HVI and LVI groups, as well as between the HVI and control groups (K-W test: $P < .0001$), but no differences were observed between the LVI and control groups in the post hoc analysis (Dunn's test: $P = .24$).

Descriptive Histopathologic Evaluation

HVI group (n = 18). In the skin, only mild histologic lesions were present in the in the superficial dermis, consisting of mild hyperemia, Average HS (AHS) = 0.61, and minimal perivascular and periadnexal inflammatory infiltration of lymphoplasmacytic cells and macrophages (AHS = 0.72).

In the lymph nodes during early acute phase (7 dpi), reactive cortical hyperplasia could be observed with karyorrhexis, karyolysis, and cell debris in the germinal center (lymphocytolysis). As the process evolved (10 dpi), there was a marked loss of lymphoid cells (lymphoid depletion), mainly in secondary lymphoid follicles, as well as a relative hyperplasia of the mononuclear phagocyte system (AHS = 1.39). In the most affected lymph nodes (gastrohepatic, renal, mesenteric, mediastinal, and ileocecal), a maximum of 15 animals (83%) presented multifocal apoptosis of lymphocytes, characterized by cell swelling with chromatin clumping, karyorrhexis, karyolysis, and cell debris in the germinal center and paracortex, with moderate to severe presence of tingible body macrophages (AHS = 1.92) (Fig. 4a and Supplemental Figures S1d-f). In severe cases, lymphoid populations were replaced by an abundant central deposit of eosinophilic cellular debris and intercellular edema. Almost all the animals of the HVI group had vascular dilatation and diffuse hyperemia in some of the most affected

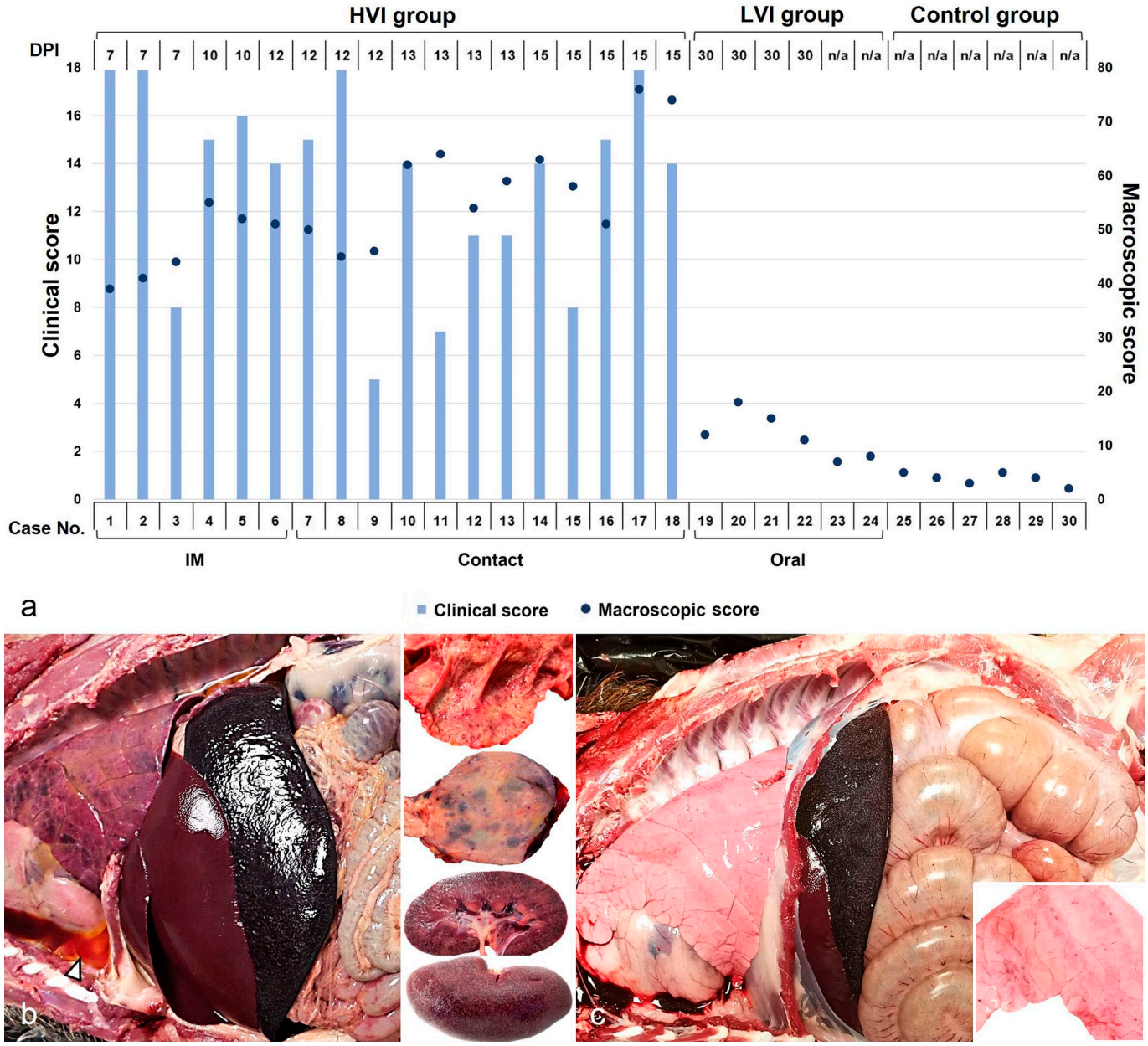

Figure 3. Clinical and macroscopic evaluation of wild boar infected with African swine fever virus. (a) Clinical score (CS) and macroscopic score (MS) obtained in each case according to the virulence isolate, days post-infection (dpi), and route of administration. MS values tended to increase as days post-infection elapse, while CS values were highly variable. The CS of each animal was obtained by summing the scores calculated through semiquantitative evaluation (0-4) of the different signs. The MS of each animal was obtained by summing the scores calculated through semiquantitative evaluation (0-3) of the different organs. IM, intramuscular. (b, c) Necropsy findings. Thoracic and abdominal cavities from (b) high virulent isolate (HVI) group and (c) low virulent isolate (LVI) group. (b) Moderate hydrothorax (arrowhead) with pulmonary edema, congestion, and multifocal subpleural hemorrhages. Hyperemia and enlargement of the spleen and liver. Multifocal hemorrhages in the mucosa of the intestine (upper right inset); the urinary bladder (middle right inset); and the medulla, cortex, and pelvis of the kidney (bottom right inset). (c) Splenic hyperemia and splenomegaly, and minimal multifocal subpleural petechial hemorrhages (bottom right inset).

lymph nodes (gastrohepatic, renal, mesenteric, mediastinal, and ileocecal). According to severity, hemorrhagic areas could be observed evolving from the subcapsular medullary zone, followed by the deeper medullary cords and the paracortex (AHS = 1.78) (Supplemental Figures S1a-c). The gastrohepatic and renal lymphatic nodes were particularly affected, with a maximum of 15 animals (83%) having severe hemorrhagic lesions affecting the entire tissue. Occasionally, there was total loss of lymphoid follicles with hemorrhages infiltrating the marginal zone and germinal centers (AHS = 2.75) (Fig. 4a and Supplemental Figure S1c).

The bone marrow displayed moderate to severe hypocellularity of myeloid and erythroid cells, with an apparent increase in the proportion of adipose tissue (>50% of the total area)

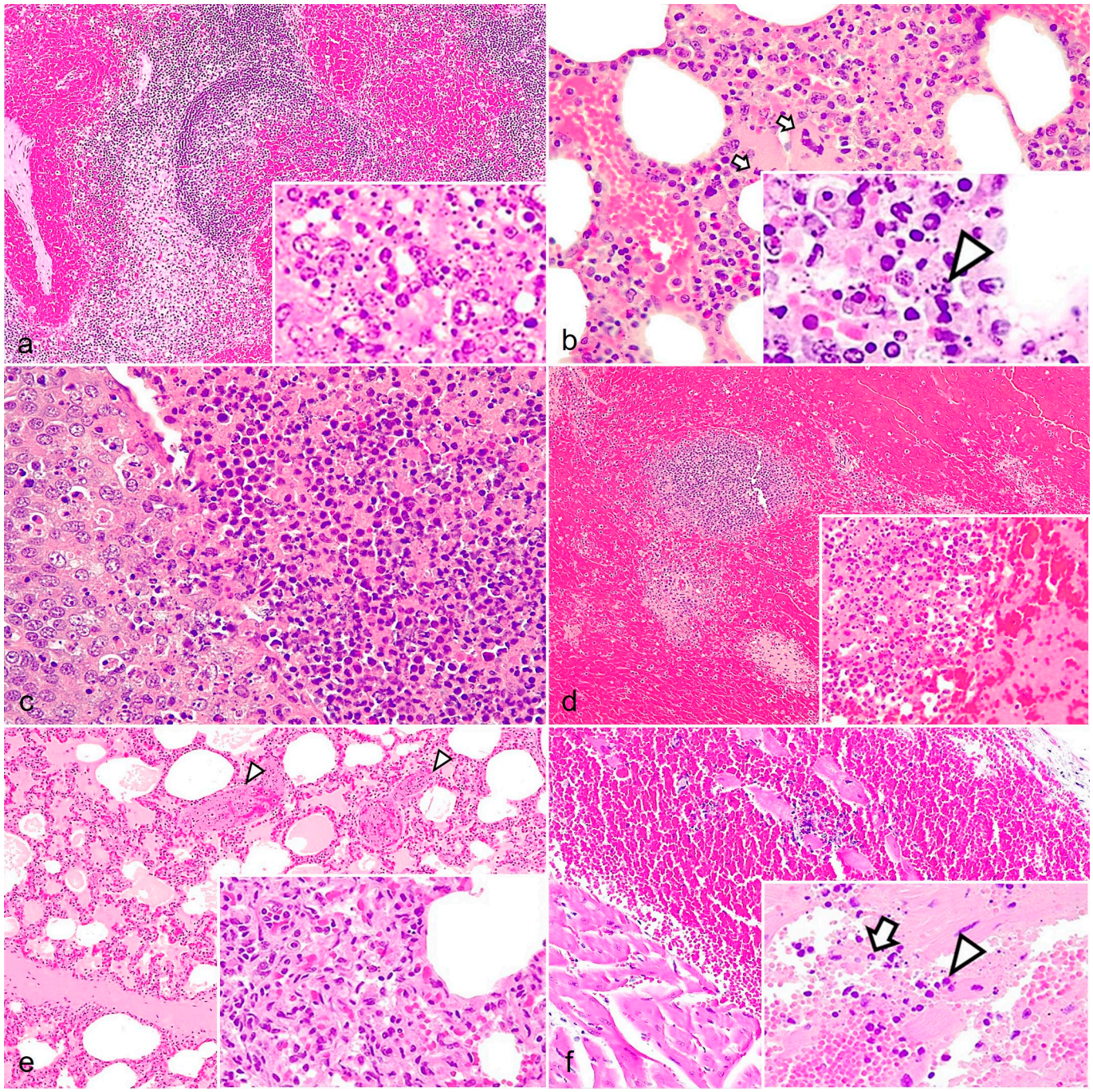

Figure 4. Histopathologic findings of acute African swine fever in wild boar. (a) Lymph nodes. Multifocal to coalescing hemorrhages in medullary cords and the cortex, infiltrating the marginal zone and the germinal center. Hematoxylin and eosin (HE). Inset: diffuse lymphoid depletion with abundant pyknotic cells and cell debris in the germinal center (lymphocytolysis). HE. (b) Bone marrow. Venule and capillary hyperemia with apoptotic megakaryocytes (arrows). Inset: nuclear fragmentation of the mononuclear cells (arrowheads). (c) Palatine tonsils. The epithelium of the crypts contains pyknotic and karyorrhectic cells, and the lumen is filled with extensive infiltrates of mononuclear and polymorphonuclear cells displaying pyknosis and karyorrhexis. HE. (d) Spleen. Diffuse congestion and hemorrhage of the splenic red pulp. The marginal zone, lymphoid follicles, and periarteriolar lymphoid sheaths are depleted, difficult to discern, and appear to be infiltrated by erythrocytes. Inset: diffuse lymphoid depletion and lymphocytolysis in the germinal center. HE. (e) Lungs. Hyperemia, alveolar and interstitial edema, and thrombosis (arrowheads). Inset: septal thickening due to capillary dilation and mononuclear inflammatory infiltrate. HE. (f) Heart. Extensive hemorrhage between the muscle fibers in the myocardium and endocardium. Inset: focal inflammation mainly composed of mononuclear infiltrates (arrowhead) and scarce number of neutrophils (arrow) and nuclear debris. HE.

(AHS = 1.78). Reduced numbers of megakaryocytes were observed (AHS = 2.11), occasionally displaying apoptotic features such as condensed chromatin, pyknosis, or karyorrhexis. Mononuclear cells also presented multifocal to diffuse pyknosis and karyorrhexis (AHS = 1.94). Moreover, diffuse hyperemia and focal to multifocal interstitial hemorrhages were observed, and 2 animals (11%), presented fibrin strands (AHS = 1.67) (Fig. 4b and Supplemental Figures S2a-c).

In the palatine tonsils, 10 wild boars (56%) had vascular dilatation and generalized hyperemia, with multifocal hemorrhages in the submucosa (AHS = 0.67). Lymphocytic depletion of mucosa-associated lymphoid tissue with mild or moderate lymphocytolysis was frequently observed, mainly in secondary lymphoid follicles (AHS = 1.50). In addition, 16 cases (89%) had foci of necrosis at the interfollicular zone and crypts (AHS = 1.44), with the presence of desquamated epithelial cells, degenerate erythrocytes, and many neutrophils in the lumen of the crypts (microabscess) (AHS = 1.61) (Fig. 4c and Supplemental Figures S3 a-c).

The thymus displayed moderate to severely decreased lymphoid cellularity. In 14 animals (78%), the cortex was atrophic with decreased thickness, pyknotic cells, and lymphocytic nuclear fragmentation with a moderate to severe number of tingible body macrophages, giving a "starry sky" appearance. The most severe cases, described in 4 animals (22%), showed loss of the cortical structure with relative hyperplasia of the medulla, and Hassall's corpuscles were evident and close to the surface of the organ (AHS = 1.83) (Supplemental Figures S4 a-c). The medulla contained moderate to severe lymphocyte karyorrhexis (AHS = 1.72). Mild to moderate hemorrhages were observed in 5 animals (28%), with focal or multifocal distribution in the cortex and/or medulla, which affected only single lobules (AHS = 0.44) (Supplemental Figures S4d-f).

In the spleen, all the animals had lymphoid depletion of the white pulp. There was relative hyperplasia of the red pulp mononuclear phagocyte system, with sinus histiocytosis, cell debris, and fibrin deposits (AHS = 1.78). In the lymphoid follicles and periarterial lymphoid sheath, we observed apoptosis of the lymphoid cells (lymphocytolysis), which appeared to be infiltrated by a moderate to severe number of tingible body macrophages (AHS = 1.83). Eleven animals (61%) had multifocal hemorrhages within the white pulp (AHS = 2.28) and, in severe cases, coagulative necrosis of the perifollicular areas and the mononuclear phagocyte system (AHS = 0.72) (Fig. 4d and Supplemental Figures S5a-c).

The lungs were diffusely hyperemic with angiectasia and thickening of alveolar septa. There was alveolar and interstitial edema (AHS = 2.17) and hemorrhages (AHS = 1.83) and perivascular, peribronchiolar, and peribronchial mononuclear infiltrates (AHS = 1.78) (Fig. 4e and Supplemental Figures S6a-c). Bronchus-associated lymphoid tissues occasionally had lymphocytic depletion with pyknosis and karyorrhexis (AHS = 1.11). We observed diffuse endothelial activation characterized by endothelial cell hypertrophy, which was, in some cases, associated with subintimal edema. Fifteen animals (83%) had total obstruction of small and medium caliber blood vessels due to the accumulation of fibrin and inflammatory cells that adhere to the vascular wall (thrombosis) that was associated with fibrinoid necrosis of the arteries and arterioles (AHS = 2.06) (Fig. 4e).

The heart of 13 animals (72%) was hyperemic and contained focal or multifocal hemorrhages in the endocardium and, less frequently, in the epicardium and myocardium (AHS = 0.94) (Fig. 4f and Supplemental Figures S7a-f). Only 4 animals (22%) displayed extensive hemorrhagic lesions (Supplemental Figures S7c, f). One case (6%) had more extensive hemorrhages in the endocardium and necrotic cardiac muscle fibers with cytoplasmic hypereosinophilia and loss of striations due to coagulative necrosis (Zenker's degeneration). Five cases (28%) had mild to moderate multifocal mononuclear interstitial inflammatory infiltrates in the endocardium, epicardium, and myocardium (AHS = 0.28) (Fig. 4f).

The kidneys had widespread vascular dilatation and congestion, with 16 cases (89%) displaying multifocal interstitial hemorrhages and edema, primarily in the cortex (AHS = 1.94) but also extending into the medulla and pelvis (AHS = 1.44) (Fig. 5a and Supplemental Figures S8a-f). Fifteen cases (83%) had mild to moderate, multifocal interstitial nephritis in the interstitium and perivascular area (AHS = 1.22) (Supplemental Figure S8b). Tubulonephrosis with an occasional deposit of hyaline material inside the lumen (hyaline casts) was observed in 3 animals (17%) (AHS = 1.00) (Supplemental Figure S8e). In moderate and severe cases, there were thrombi in the glomerular blood vessels (indicative of disseminated intravascular coagulation) and fibrinonecrotic glomerulonephritis (Supplemental Figure S8f). Urinary bladders had hyperemia of the mucosa, lamina propria, muscularis, and serosal layers, with edema in the lamina propria. In 12 cases (67%), multifocal hemorrhages of varying severities were present in the mucosa (AHS = 0.72) (Fig. 5b and Supplemental Figures S9a-c). Six animals (33%) had mild perivascular lymphocytic infiltration in the lamina propria (AHS = 0.28).

In the liver, we observed multifocal vascular dilatation mainly in the portal triad and the centrolobular sinusoids due to congestion. Severe cases had centrilobular coagulative necrosis that extended to zone 2 of the hepatic acinus (AHS = 1.56) (Fig. 5c and Supplemental Figures S10a-c). In addition, there was partial obstruction of blood vessels by fibrin thrombi. Multifocal lymphoplasmacytic infiltrates were present in portal tracts and interlobular septa (Fig. 5c). Hepatic sinusoids contained increased numbers of lymphocytes and prominent Kupffer cells, undergoing a process of swelling (AHS = 1.50). Eleven cases (61%) had marked thickening of the gallbladder wall due to severe edema in the lamina propria and muscularis layers with multifocal mucosal hemorrhages of varying severity (AHS = 0.83).

Hyperemia was present in the gastric mucosa, submucosa, and serosa, but was most severe in the apical part of the lamina propria. In 7 cases (39%), there were multifocal hemorrhages and mucosal ulceration (AHS = 1.33) (Supplemental Figures S11a-c). A diffuse mononuclear inflammatory infiltrate was noted within the lamina propria and perivascularly in the

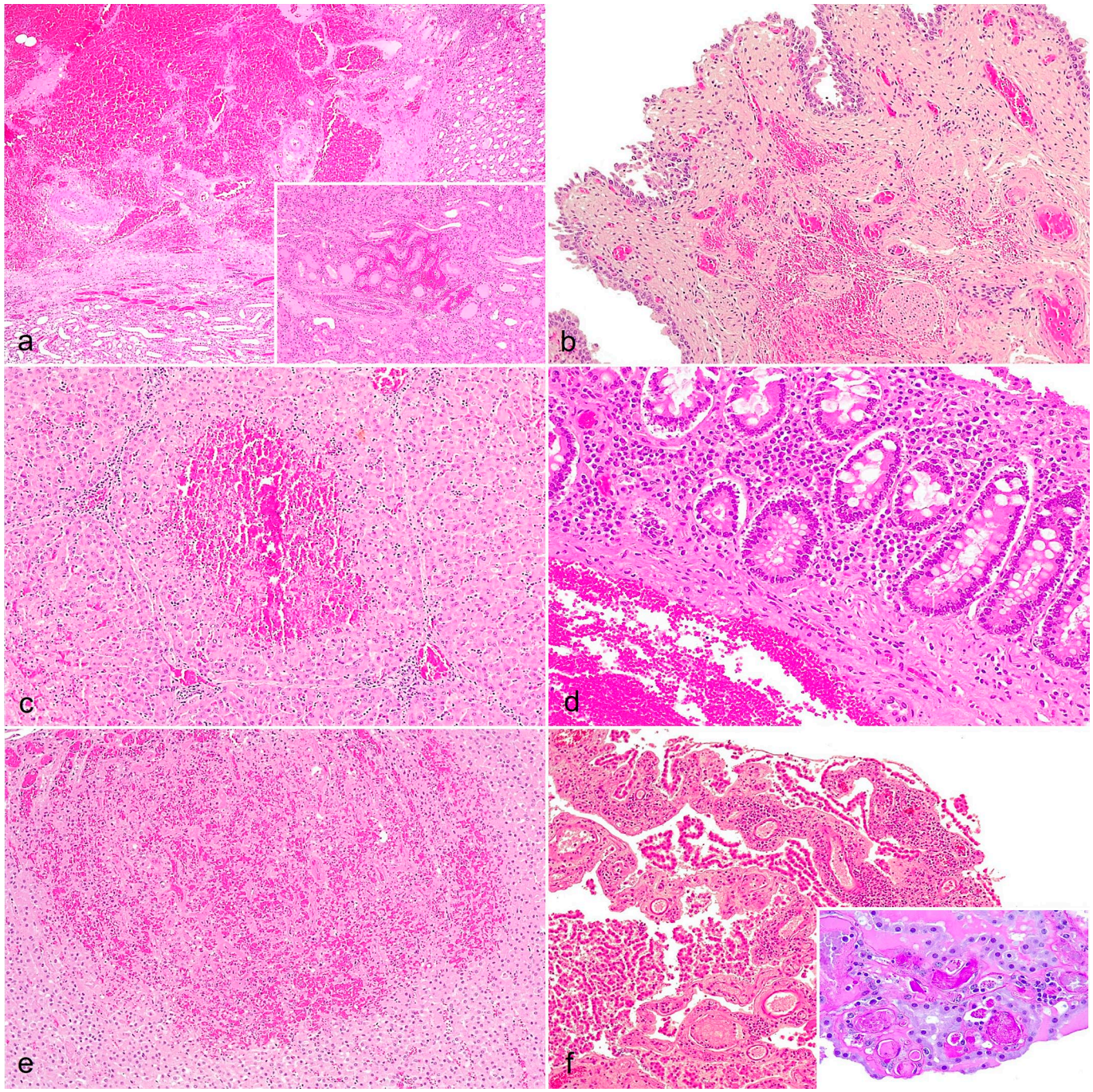

Figure 5. Histopathologic findings of acute African swine fever in wild boar. (a) Kidneys. Multifocal interstitial hemorrhages in the medulla and renal pelvis. Hematoxylin and eosin (HE). Inset: interstitial cortical hemorrhage. HE. (b) Urinary bladder. Hyperemia and multifocal submucosal hemorrhages. HE. (c) Liver. Congestion and focally extensive hemorrhage of the hepatic acinus with centrilobular and midzonal coagulative necrosis. Multifocal periportal mononuclear inflammation. HE. (d) Large intestine. Increased lymphoplasmacytic cellularity of the lamina propria and submucosal hemorrhage. HE. (e) Adrenal glands. Congestion and cortical hemorrhage. HE. (f) Brain (choroid plexus). Congestion and multifocal mononuclear inflammation. HE. Inset: the bright magenta-stained deposits in the vascular lumen demonstrate the presence of thrombi. Periodic acid-Schiff reaction.

submucosa. Ten animals (56%) displayed moderate to severe hyperplasia of the lymphoid tissue, predominantly in the cardia (gastric mucosa-associated lymphoid tissue) (follicular chronic gastritis), and occasionally lymphocytic depletion with pyknosis and karyorrhexis in germinal centers (AHS = 2.28) (Supplemental Figures S11d-f).

Small intestinal villi were frequently atrophied and fused, and crypts were with hyperplastic and dilated. The mucosa, submucosa, and serosa were hyperemic, but hyperemia was most severe in the apical part of the villi (Supplemental Figure S12b). Seven cases (39%) had multifocal hemorrhages in the lamina propria and the submucosa, and less frequently, in

severe cases, ulceration of the mucosa (AHS = 1.44) (Supplemental Figures S12b-c). We observed diffuse lymphoplasmacytic infiltrates in the lamina propria and multifocal perivascular infiltrates in the submucosa (AHS = 1.72) (Supplemental Figures S12a-c). In addition, 11 cases (61%) had hyperplasia of intestinal-associated lymphoid tissues in the ileum, occasionally with lymphocytic depletion with pyknosis and karyorrhexis (AHS = 0.89).

The large intestines were diffusely hyperemic and there were multifocal hemorrhages of the lamina propria and less frequently in the submucosa in 6 cases (33%) (Fig. 5d and Supplemental Figures S13a-c). Ulceration of the mucosa was rarely found (AHS = 1.28). Diffuse lymphoplasmacytic infiltrates were frequently observed in the lamina propria and multifocal perivascular infiltrates were observed in the submucosa (AHS = 1.50). Fourteen animals (78%) had intestinal-associated lymphoid tissue hyperplasia, occasionally with lymphocytic depletion with pyknosis and karyorrhexis (AHS = 1.00).

The adrenal glands had slight vascular dilatation and congestion with occasional perivascular edema. Less frequently, in moderate and severe cases, multifocal extensive hemorrhages were observed in the cortex and medulla, with occasionally foci of necrosis, mainly in the *zona fasciculata* and *zona reticularis* (AHS = 1.28) (Fig. 5e and Supplemental Figures S14a-c). A mild lymphocytic perivascular infiltrate was infrequently present (AHS = 0.17).

In the pancreas, we observed vascular dilatation and hyperemia with perivascular edema in the interstitium of the perilobular septa. Fifteen cases (83%) had multifocal hemorrhages of varying severity, and moderate or severe cases (50%) had areas of necrosis in pancreatic acini (AHS = 1.50) (Supplemental Figures S15b-c). In addition, 14 animals (78%) had mild or moderate multifocal mononuclear and neutrophilic infiltrates in perivascular and periductal areas (AHS = 0.89) (Supplemental Figures S15a-b).

Brains had moderate vascular dilatation and congestion, which was more pronounced in the meninges and the choroid plexus, where 5 animals (29%) had perivascular hemorrhages and edema (AHS = 1.22). Sixteen animals (89%) had inflammatory infiltrates in the meninges and choroid plexus, which was primarily composed of lymphocytes, plasma cells, macrophages, and eosinophils accompanied by pyknotic cells and cell debris deposit (AHS = 1.61) ((Fig. 5f and Supplemental Figures S16a-c). Perivascular cuffs were observed in all animals (100%) in the cerebral and cerebellar neuroparenchymal, which were primarily composed of lymphocytes, plasma cells, macrophages, and cellular debris with pyknotic cells (AHS = 2.17) (Supplemental Figures S16d-f). Blood vessels in affected areas had endothelial activation and severely affected vessels contained thrombi (AHS = 1.50) (Fig. 5f). Affected areas had increased glial cells, including increased oligodendrocytes (satellitosis) and microglia (neuronophagia) around the neurons.

No hemorrhagic or inflammatory lesions were observed in the female reproductive tract (ovaries and uterus) (AHS = 0).

LVI group (n=6). The histopathologic study revealed non-specific lesions and minimal vascular changes in LVI-infected boar, which primarily consisted of congestion and mild extravasation of the erythrocytes in some lymph nodes (retropharyngeal, gastrohepatic, renal, and mesenteric) (AHS = 0.19), thymus (AHS = 0.67), lungs (AHS = 0.67), liver (AHS=AHS = 1.17), spleen (AHS = 0.83), stomach (AHS = 0.83), intestines (AHS = 1.00), and brain (AHS = 0.67). In addition, these animals displayed mild mononuclear inflammatory infiltration in the tonsils (AHS = 0.83), lung (AHS = 0.33), liver (AHS = 0.50), kidney (AHS = 0.33), urinary bladder (AHS = 0.50), and gastrointestinal tract (AHS = 1.22).

Round to ovoid, well-defined perivascular immune cell aggregates composed of lymphocytes were associated with the mucosa, mainly in the kidney (renal hilum), but also in the esophagus, urinary bladder, and gallbladder. Moreover, some animals had minimal apoptosis of the lymphocytes in some lymphoid tissues, mainly affecting the germinal centers in lymph nodes (AHS = 0.46), tonsils (AHS = 0.50), and spleen (AHS = 0.83). However, this lesion was frequently accompanied by a moderate number of mitoses located in the germinal centers. On the other hand, the thymus displayed minimal cortical atrophy with a small number of tingible body macrophages (AHS = 0.67), and the bone marrow contained a mild elevation in the myeloid-to-erythroid ratio (indicative of relative myeloid hyperplasia) attributed to an increased number of granulocytic cells (AHS = 1.17), and mild reduction in megakaryocyte number (AHS = 0.50).

We found significant statistical differences (Dunn's test: $P \leq .01$) in the severity of certain evaluated parameters in the HVI group compared to the LVI group, including an increased severity in hemorrhages in lymph nodes (inguinal, submandibular, mediastinal, gastrohepatic, renal, mesenteric, and ileocecal), bone marrow, lungs, heart, spleen, kidneys and brain; lymphoid depletion and lymphocytolysis in lymph nodes (retropharyngeal, submandibular, mediastinal, gastrohepatic, renal, mesenteric, and ileocecal), bone marrow, and thymus; and inflammatory infiltrates in the tonsil, lungs, liver and brain in the HVI group.

Control group (n=6). The histopathologic examination revealed non-specific lesions and minimal vascular alterations, predominantly congestion and mild extravasation of erythrocytes, in certain lymph nodes (retropharyngeal, renal, mediastinal, and mesenteric) (AHS = 0.35), lungs (AHS = 0.33), spleen (AHS = 1.00), and liver (AHS = 1.33). In addition, these animals had mild inflammatory infiltrates in the tonsils (AHS = 0.83), lung (AHS = 0.17), and liver (AHS = 0.17).

Significant statistical differences (K-W test: $P \leq .05$) were found in the severity of almost all parameters in the HVI group compared to the control group (Dunn's test: $P \leq .05$), except for congestive/ hemorrhagic lesions in the skin, tonsils, thymus, liver, urinary bladder, uterus, and ovaries; and inflammatory infiltrates in the heart, adrenal gland, and urinary bladder.

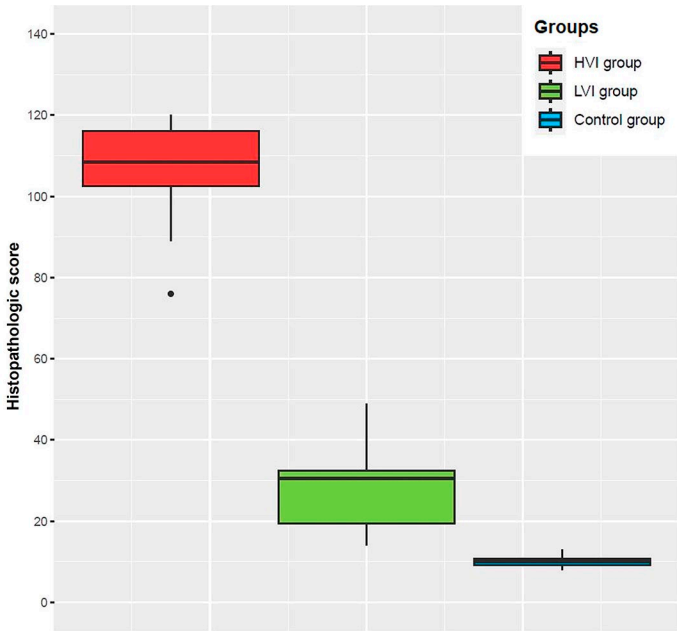

Figure 6. Histopathologic score (HS) obtained in each group, high virulent isolate (HVI) = red color; low virulent isolate (LVI) = green color; control = blue color. Boxes indicate the interquartile range, middle highlighted bars inside boxes indicate median values, and the top and bottom of the box indicates the 75th and 25th percentile. Whiskers denote 97.5th and 2.5th percentile. The HS of each animal was obtained by summing the scores calculated through semiquantitative evaluation (0-3) of the different organs.

Furthermore, there were almost no significant statistical differences (Dunn's test: $P > .05$) in the severity of the parameters evaluated in the LVI group compared to the control group, except for congestive/ hemorrhagic lesions in the stomach and intestine, and inflammatory infiltrates in the intestines (Dunn's test: $P \leq .05$).

HS Statistical Analysis

The HS differed significantly between the HVI, LVI, and control groups (K-W test: $P < .0001$). As expected, the HVI group had the highest total score (109.3; 95% CI: 103.7-115), while the LVI group had a much lower score (28.8; 95% CI: 18.6-39), and the negative control group's score was even lower (9.7; 95% CI: 8.4-11) (Fig. 6). There were no significant differences in the HS between HVI subgroups (M-W test: $P = .37$). Animals that were IM-infected had an AHS of 104 (95% CI: 89.8-118.2), while those that were contact-infected had an AHS of 112 (95% CI: 107.5-116.5). Individual HS values for each tissue and animal evaluated are shown in Fig. 7. Median HS values for each tissue evaluated in the different groups are shown in Supplemental Table S21. Individual HS values for each evaluated parameter in every tissue are provided in Supplemental Table S22.

A positive correlation was observed between HS and dpi, but, in contrast to the MS, it was moderate (r = 0.55, CI: 0.11-0.81). Also, there was a strong positive correlation between the HS and MS obtained for each animal (r = 0.97, CI: 0.93-0.99), as well as between HS and MS obtained from individual parameters, including hemorrhage, edema, and necrosis (r = 0.76, 95% CI: 0.72-0.79). Regarding viral loads, a strong negative correlation was observed between total HS and Ct in blood samples, r = -0.96, 95% CI: -0.92-, -)0.98), as well as a moderate negative correlation between HS and Ct in tissue samples, r = -0.68, 95% CI: -0.63-, -)0.73). Furthermore, there was a strong positive correlation between total HS and CS (r = 0.84, 95% CI: 0.69-0.92).

Discussion

Scarce studies have evaluated the pathology of ASF, and even fewer in wild boar, with most of them focusing on macroscopic evaluations. While macroscopic investigations are an essential source of information and are necessary for early diagnosis, especially in dead animals found in the field, it can be incomplete, limited, and sometimes misinterpreted. Our results indicate strong correlations between MS and HS, highlighting the need for both methods in understanding ASF pathology. However, the histopathologic study of ASF provides more specific information, especially on the state of the lymphoid cells, that is, the immune status of the animal.

No single lesion may lead to a proper diagnosis, and a comprehensive histopathologic evaluation is needed, with especial attention to certain lesions as follows: (a) lymphoid depletion/ lymphocytolysis in the spleen and lymph nodes; (b) vascular alterations in the lymph nodes (principally gastrohepatic and renal), spleen, lungs, liver, kidneys, and brain (particularly in the choroid plexus); and (c) mononuclear inflammatory infiltrates in the lungs, liver, and brain, and necrotizing tonsillitis.

Based on previous histopathologic studies,[18,21,31,34,35,39] we observed no significant differences between domestic pigs and wild boar, in the main target organs for ASFV (spleen, lung, liver, and kidney).[12] However, there are certain findings in other organs that should be mentioned. It seems that skin alterations in wild boar are much less frequent than in domestic pigs, in which vascular, necrotic and inflammatory lesions are more variable and severe in acute/subacute forms.[34] Macroscopically, it could be partly attributed to the broader coat compared to domestic pigs.[27] This handicap can lead to a misinterpretation of the lesions, observing that most of the cases macroscopically interpreted as hemorrhages were only hyperemic areas, confirmed by light microscopy. Moreover, extensive hemorrhagic lesions with coagulative necrosis of muscle fibers have been previously described in domestic pigs,[34] suggesting a higher frequency and severity compared to wild boars. Petechial and extensive hemorrhages in the urinary bladder and gastrointestinal tract have been previously described macroscopically as possible acute or subacute lesions.[27,34,37] However, to our knowledge, until our study, these lesions had not been histopathologically described and graded in wild boar. There was variability in the appearance and severity of these lesions, which could be related to stress and immune factors, where secondary infections may also

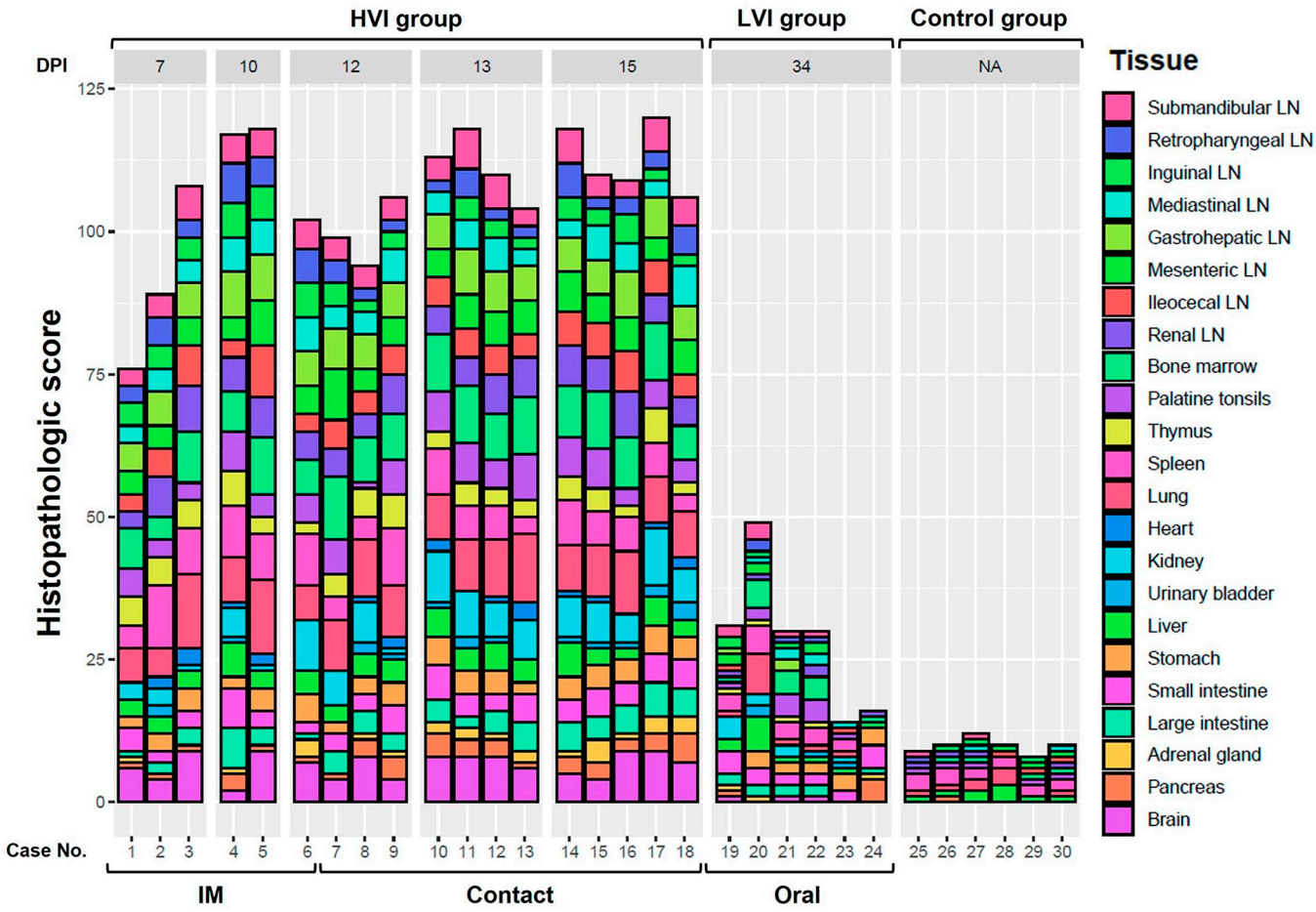

Figure 7. Histopathologic score (HS) in each animal and tissue, obtained according to the group (high virulent isolate [HVI], low virulent isolate (LVI), and control group), virulence isolate, days post-infection (DPI), and route of administration. The HS of each animal and tissue was obtained by summing the scores calculated through semiquantitative evaluation (0-3) of the different tissues. IM, intramuscular; LN, lymph node.

contribute.[27] We identified specific lesions that have been rarely described in the ASF histopathology literature,[34,37] particularly hemorrhagic/ necrotic foci in the pancreas and hemorrhages in the adrenal glands. When interpreting the lesions in the pancreas, caution is crucial, as it might be challenging to distinguish them from cases involving intrapancreatic accessory spleens, particularly in instances of intense lymphoid depletion.[23] In the brain, non-purulent meningoencephalitis was noted and was characterized by the presence of inflammatory cell infiltrates in the meninges and choroid plexus, as well as neuroparenchymal perivascular cuffs with neuronal necrosis and gliosis. These findings, also observed in naturally infected wild boar,[37] are consistent with previous studies in domestic pigs.[18,34] This findings support the hypothesis that proinflammatory cytokines contribute to inflammatory lesions in the brain.[18] Finally, information on lesions and distribution of ASFV in the reproductive system is scarce. We have not observed any significant lesions affecting the ovary and uterus, in contrast to the hemorrhages in the vaginal vestibule in wild boar described elsewhere.[37] However, vascular alterations of the epididymis, testis, prostate, and vesicular gland were observed in domestic pigs and wild boar,[21,34,37,38] suggesting higher susceptibility in male reproductive organs.

It is important to note that certain hemorrhagic lesions, such as in the skin, heart, urinary bladder, and reproductive tract, did not show statistically significant differences compared to the control group. These results suggested that the animals studied did not develop a complete subacute form of the disease, characterized by more extensive hemorrhagic and edematous lesions. Wild boars infected with the HVI, exhibited a survival duration of 7-15 dpi, predominantly displayed acute lesions, along with characteristic lesions indicative of the onset of the subacute form. Contact-infected animals had an average survival time of 12-15 dpi, in contrast to IM-infected animals, which exhibited an average survival time of 7 to 12 dpi, as expected due to the incubation period. In addition, there was a positive correlation for MS and HS with elapsed dpi. According to the descriptive results, severe and extensive hemorrhagic lesions in certain organs (kidney, heart, gallbladder, urinary bladder, adrenal gland, and pancreas) appeared between 10 and 12 dpi in IM-infected animals, whereas in contact-infected animals, these findings were observed between 13 and 15 dpi.

The clinical course, histopathologic findings, and the presence of viral genome in tissues did not exhibit variance between the 2 subgroups (IM- and contact-infected), suggesting that the infection route does not play a decisive role in the pathological course of HVI. However, this cannot be confirmed, as the infection dose in the contact-infected subgroup cannot be specified, and therefore, it is not perfectly comparable. Conversely, a moderate correlation was observed between HS and CS, as well as between HS and viral loads (strong for blood and moderate for tissues). However, correlations did not reach statistical significance when considering only animals in the HVI group. These results highlight the individual variability within the HVI group regarding the severity of lesions, clinical signs, and viral loads. This fact also suggests that although viral clearance occurs, the severity of the lesions in some organs persists for a longer period of time. In contrast, other organs, such as the heart and urinary bladder, exhibited high viral loads; nevertheless, most of the cases showed no lesions or had mild lesions in these organs.

When ASFV enters disease-free areas, the clinical presentation and pathological findings are consistent acute and subacute disease in most infected animals.[16] However, when ASFV is established in an area, the disease can eventually evolve to unapparent clinical forms,[14,16] as observed in the animals of our study infected with the attenuated Lv17/WB/Rie1 ASFV isolate. In the LVI group, minimal lesions were observed and were characterized by lymphocyte apoptosis in the lymphoid organs with inflammation, congestion/ hyperemia and, rarely, hemorrhages in several organs. These lesions were more frequent and severe in case 19, which had a higher viral load in blood and yielded positive PCR results in all sampled tissues. The hyperemic lesions discussed above could be due, in part, to vasodilation caused by the barbiturate overdose given during euthanasia, since no statistically significant differences were observed compared to the control group, especially in the spleen and liver. It is important to mention that the lymphoid cell aggregates were mainly located in the renal calyx, close to the urothelium. These formations, compatible with tertiary lymphoid structures, have recently been described in wild boars infected with a low virulence isolate of ASF, and could function in the local protective response, emulating the role of mucosa-associated lymphoid tissues.[24]

The activation of monocytes and macrophages produces proinflammatory cytokines, causing apoptosis of lymphocytes in the lymphoid tissue.[28,29,34] This mechanism appears to be activated minimally and in a short period of time in the LVI group. Lymphocytolysis may have resolved in a recovery period after the peak of virulence, as we observed increased mitosis mainly in the germinal center of lymphoid follicles, possibly due to a natural immune response. In addition, as described above, this group had mild hyperemic/ hemorrhagic lesions, although we did not observe a clear correlation with the presence of the virus. This could be compatible with an acute-transient course of infection with early virus clearance,[19] but without expressing compatible clinical signs. Nonetheless, a recent study on pigs infected with low virulence variants of ASFV from outbreaks in the South Caucasus also reported isolated microhemorrhages and diapedesis of erythrocytes.[3] Furthermore, we have not seen similarities with other experimental infections with low virulent ASFV isolates focused on studying or inducing chronic forms. These chronic forms may include fibrinous and necrotic lesions mainly in pleura and pericardium, but also in joints and skin.[34,36] Such lesions are due to immunosuppression over a prolonged period of time, which favors secondary bacterial co-infection.[28,34,36] Moreover, recent studies in IM- and contact-infected domestic pigs inoculated with a lower dose of the Lv17/WB/Rie1 isolate, observed fibrinous pericarditis and focal pneumonia at 25 and 45 dpi.[14] This fact contrasts with our study, where no such lesions were observed, and the immune system was only mildly compromised over a short period of time. This may suggests that the oronasal route enhances protection, due to absorption of the virus through the oral and upper respiratory mucosa, exposing it to innate defense mechanisms.[17,30,31] These results are being pursued in experimental studies with live attenuated isolates in order to develop an effective and safe vaccine prototype,[4,5] and the fact that the HS is closer to the negative controls is positive from this point of view. Comparing the 2 infected groups (HVI and LVI), we can suggest that depending on the virulence of the strain, the route of administration may influence, to a greater or lesser extent, the presence and severity of lesions. However, it is important to understand that such findings are highly dependent on the animal health status, environmental factors, and other external variables.[20,33] Further long-term experimental studies should be conducted to assess the development of possible chronic lesions.

It is important to highlight that the comparison of the different virus isolates posed challenges due to the inconsistent use of the same route of administration in both groups. Similarly, we acknowledge the limitation of using only 30 animals, exclusively females, as we have not been able to thoroughly assess potential lesions in the male reproductive system. Likewise, we have only included animals of the same age (3-4 months), mainly due to the handling difficulties involved in conducting experimental studies with older animals. Thus, we had to be aware of the inherent limitations of these studies, and the animal welfare requirements for their experimental design. Pathology studies had to be tailored to meet the requirements of vaccine trials; however, the availability of a gradient of isolates and routes of administration may be beneficial in developing a more consistent histopathology evaluation system. In conclusion, this new histopathologic scoring system has elucidated very useful information to our understanding of ASF pathogenesis in wild boar infected with different virulent isolates. This study paves the way for new research in the future and will serve as a tool to improve the evaluation of the efficacy and safety of vaccines and to further study their underlying mechanisms of protection.

Acknowledgments

The authors thank all those who participated in the development of this study, the sampling and data collection, especially the SUAT and

VISAVET teams. The authors also thank the technicians of the VISAVET Health Surveillance Center Pathology and Forensic Veterinary Unit, G. Torre and L. Mamblona. Sally Newton, for her English language services.

Declaration of Conflicting Interests

The author(s) declared no potential conflicts of interest with respect to the research, authorship, and/or publication of this article.

Funding

The author(s) disclosed receipt of the following financial support for the research, authorship, and/or publication of this article: This research was funded by European Project H2020 VACDIVA—"A Safe DIVA vaccine for African Swine Fever control and eradication," Grant Agreement no. 862874. JAB is a recipient of a 'Ramón y Cajal' contract (RYC2022-038060-I) funded by the Spanish Ministry of Science and Innovation (MCIN/AEI) and Fondo Social Europeo Plus (FSE+).

ORCID iDs

Néstor Porras https://orcid.org/0000-0002-2876-8850
José Á. Barasona https://orcid.org/0000-0003-4066-8454
Alberto Gómez-Buendía https://orcid.org/0000-0002-8968-0836

References

1. Alonso C, Borca M, Dixon L, et al. ICTV Report Consortium. ICTV virus taxonomy profile: asfarviridae. *J Gen Virol*. 2018;**99**:613–614.
2. Arias M, Jurado C, Gallardo C, et al. Gaps in African swine fever: analysis and priorities. *Transbound Emerg Dis*. 2018;**65**:235–247.
3. Avagyan H, Hakobyan S, Baghdasaryan B, et al. Pathology and clinics of naturally occurring low-virulence variants of African swine fever emerged in domestic pigs in the south caucasus. *Pathogens*. 2024;**13**:130.
4. Barasona JA, Cadenas-Fernández E, Kosowska A, et al. Safety of African swine fever vaccine candidate Lv17/WB/Rie1 in wild boar: overdose and repeated doses. *Front Immunol*. 2021;**12**:761753.
5. Barasona JA, Gallardo C, Cadenas-Fernández E, et al. First oral vaccination of Eurasian wild boar against African swine fever virus genotype II. *Front Vet Sci*. 2019;**6**:137.
6. Blome S, Gabriel C, Beer M. Pathogenesis of African swine fever in domestic pigs and European wild boar. *Virus Res*. 2013;**173**:122–130.
7. Cadenas-Fernández E, Sánchez-Vizcaíno JM, Kosowska A, et al. Adenovirus-vectored African swine fever virus antigens cocktail is not protective against virulent Arm07 isolate in Eurasian wild boar. *Pathogens*. 2020;**9**:171.
8. Chenais E, Ståhl K, Guberti V, et al. Identification of wild boar-habitat epidemiologic cycle in African swine fever epizootic. *Emerg Infect Dis*. 2018;**24**:810–812.
9. European Commission Joint Research Centre; Coelho Cruz B, Toussaint B, et al. *African Swine Fever (ASF) Vaccine Development: Progress and Challenges*. Luxembourg: Publications Office of the European Union; 2023.
10. Fernández-Pinero J, Gallardo C, Elizalde M, et al. Molecular diagnosis of African Swine Fever by a new real-time PCR using universal probe library. *Transbound Emerg Dis*. 2013;**60**(1):48–58.
11. Gabriel C, Blome S, Malogolovkin A, et al. Characterization of African swine fever virus Caucasus isolate in European wild boars. *Emerg Infect Dis*. 2011;**17**:2342–2345.
12. Galindo-Cardiel I, Ballester M, Solanes D, et al. Standardization of pathological investigations in the framework of experimental ASFV infections. *Virus Res*. 2013;**173**:180–190.
13. Gallardo C, Nieto R, Soler A, et al. Assessment of African swine fever diagnostic techniques as a response to the epidemic outbreaks in eastern European Union countries: how to improve surveillance and control programs. *J Clin Microbiol*. 2015;**53**:2555–2565.
14. Gallardo C, Soler A, Nurmoja I, et al. Dynamics of African swine fever virus (ASFV) infection in domestic pigs infected with virulent, moderate virulent and attenuated genotype II ASFV European isolates. *Transbound Emerg Dis*. 2021;**68**:2826–2841.
15. Gallardo C, Soler A, Rodze I, et al. Attenuated and non-haemadsorbing (non-HAD) genotype II African swine fever virus (ASFV) isolated in Europe, Latvia 2017. *Transbound Emerg Dis*. 2019;**66**:1399–1404.
16. Gallardo MC, Reoyo ADLT, Fernández-Pinero J, et al. African swine fever: a global view of the current challenge. *Porc Health Manag*. 2015;**1**:21.
17. Howey EB, O'Donnell V, de Carvalho Ferreira HC, et al. Pathogenesis of highly virulent African swine fever virus in domestic pigs exposed via intraoropharyngeal, intranasopharyngeal, and intramuscular inoculation, and by direct contact with infected pigs. *Virus Res*. 2013;**178**:328–339.
18. Izzati UZ, Inanaga M, Hoa NT, et al. Pathological investigation and viral antigen distribution of emerging African swine fever in Vietnam. *Transbound Emerg Dis*. 2021;**68**:2039–2050.
19. Petrov A, Forth JH, Zani L, et al. No evidence for long-term carrier status of pigs after African swine fever virus infection. *Transbound Emerg Dis*. 2018;**65**:1318–1328.
20. Pietschmann J, Guinat C, Beer M, et al. Course and transmission characteristics of oral low-dose infection of domestic pigs and European wild boar with a Caucasian African swine fever virus isolate. *Arch Virol*. 2015;**160**:1657–1667.
21. Pikalo J, Schoder ME, Sehl J, et al. The African swine fever virus isolate Belgium 2018/1 shows high virulence in European wild boar. *Transbound Emerg Dis*. 2020;**67**:1654–1659.
22. Pikalo J, Zani L, Hühr J, et al. Pathogenesis of African swine fever in domestic pigs and European wild boar—lessons learned from recent animal trials. *Virus Res*. 2019;**271**:197614.
23. Porras N, Chinchilla B, Rodríguez-Bertos A, et al. Intrapancreatic accessory spleens in African swine fever infection of wild boar (Sus scrofa). *Front Vet Sci*. 2023;**10**:1306320.
24. Porras N, Sánchez-Vizcaíno JM, Rodríguez-Bertos A, et al. Tertiary lymphoid organs in wild boar exposed to a low-virulent isolate of African swine fever virus. *Vet Q*. 2024;**44**:1–13.
25. Post J, Weesendorp E, Montoya M, et al. Influence of age and dose of African swine fever virus infections on clinical outcome and blood parameters in pigs. *Viral Immunol*. 2017;**30**:58–69.
26. R Core Team. *R: A Language and Environment for Statistical Computing*. Vienna, Austria: R Foundation for Statistical Computing; 2023. Accessed July 2, 2024. https://www.R-project.org/.
27. Rodríguez-Bertos A, Cadenas-Fernández E, Rebollada-Merino A, et al. Clinical course and gross pathological findings in wild boar infected with a highly virulent isolate of African swine fever virus genotype II. *Pathogens*. 2020;**9**:688.
28. Salguero FJ. Comparative pathology and pathogenesis of African swine fever infection in swine. *Front Vet Sci*. 2020;**19**:282.
29. Salguero FJ, Ruiz-Villamor E, Bautista MJ, et al. Changes in macrophages in spleen and lymph nodes during acute African swine fever: expression of cytokines. *Vet Immunol Immunopathol*. 2002;**90**:11–22.
30. Sánchez-Cordón PJ, Chapman D, Jabbar T, et al. Different routes and doses influence protection in pigs immunised with the naturally attenuated African swine fever virus isolate OURT88/3. *Antivir Res*. 2017;**138**:1–8.
31. Sánchez-Cordón PJ, Floyd T, Hicks D, et al. Evaluation of lesions and viral antigen distribution in domestic pigs inoculated intranasally with African swine fever virus Ken05/Tk1 (genotype X). *Pathogens*. 2021;**10**:768.
32. Sánchez-Cordón PJ, Montoya M, Reis AL, et al. African swine fever: a re-emerging viral disease threatening the global pig industry. *Vet J*. 2018;**233**:41–48.
33. Sánchez-Cordón PJ, Nunezm A, Neimanism A, et al. African swine fever: disease dynamics in wild boar. Experimentally infected with ASFV isolates belonging to genotype I and II. *Viruses*. 2019;**11**:852.
34. Sánchez-Cordón PJ, Vidaña B, Neimanis A, et al. Pathology of African swine fever. In: Iacolina L, Penrith ML, Bellini S, Chenais E, Jori F, Montoya M,

Ståhl K, Gavier-Widén D, eds. *Understanding and Combatting African Swine Fever*. Wageningen, The Netherlands: Wageningen Academic Publishers; 2021:87–139.

35. Sánchez-Vizcaíno JM, Laddomada A, Arias ML. African swine fever virus. In: Zimmerman JJ, Karriker LA, Ramirez A, Schwartz KJ, Stevenson GW, Zhang J, eds. *Diseases of Swine*. Hoboken, NJ: Wiley; 2019:443–452.
36. Sánchez-Vizcaíno JM, Mur L, Gomez-Villamandos JC, et al. An update on the epidemiology and pathology of African swine fever. *J Comp Pathol*. 2015;**152**:9–21.
37. Sehl-Ewert J, Deutschmann P, Breithaupt A, et al. Pathology of African swine fever in wild boar carcasses naturally infected with German virus variants. *Pathogens*. 2022;**11**:1386.
38. Sehl-Ewert J, Friedrichs V, Carrau T, et al. Pathology of African swine fever in reproductive organs of mature breeding boars. *Viruses*. 2023;**15**(3):729.
39. Sehl-Ewert J, Pikalo J, Schäfer A, et al. Comparative pathology of domestic pigs and wild boar infected with the moderately virulent African swine fever virus isolate "Estonia 2014." *Pathogens*. 2020;**9**:662.
40. World Organisation for Animal Health. Terrestrial animal health code. Terrestrial code online access. Accessed February 15, 2023. https://www.woah.org/en/what-we-do/standards/codes-and-manuals/terrestrial-code-online-access/.
41. World Organisation for Animal Health. World Animal Health Information System. Accessed February 15, 2023. https://wahis.woah.org/.
42. Zhang H, Zhao S, Zhang H, et al. Vaccines for African swine fever: an update. *Front Microbiol*. 2023;**14**:1139494.